Granulosa Cell-Specific Androgen Receptors Are Critical Regulators of Ovarian Development and Function

Aritro Sen and Stephen R. Hammes

Division of Endocrinology and Metabolism, Department of Medicine, University of Rochester Medical Center, Rochester, New York 14642

The physiological significance of androgens in female reproduction was unclear until female mice with global knockout of androgen receptor (AR) expression were found to have reduced fertility with abnormal ovarian function. However, because ARs are expressed in a myriad of reproductive tissues, including the hypothalamus, pituitary, and various ovarian cells, the role of tissue-specific ARs in regulating female fertility remained unknown. To examine the importance of ovarian ARs in female reproduction, we generated granulosa cell (GC)- and oocyte-specific AR-knockout (ARKO) mice by crossing AR-flox mice with MisRIIcre (GC-specific) or growth differentiation factor growth differentiation factor-9cre (oocyte-specific) mice. Relative to heterozygous and wild-type mice, GC-specific ARKO mice had premature ovarian failure and were subfertile, with longer estrous cycles and fewer ovulated oocytes. In addition, ovaries from GC-specific knockout mice contained more preantral and atretic follicles, with fewer antral follicles and corpus lutea. Finally, *in vitro* growth of follicles from GC-specific AR-null mice was slower than follicles from wild-type animals. In contrast to GC-specific AR-null mice, fertility, estrous cycles, and ovarian morphology of oocyte-specific ARKO mice were normal, although androgens no longer promoted oocyte maturation in these animals. Together, our data indicate that nearly all reproductive phenotypes observed in global ARKO mice can be explained by the lack of AR expression in GCs. These GC-specific ARs appear to promote preantral follicle growth and prevent follicular atresia; thus they are essential for normal follicular development and fertility. (*Molecular Endocrinology* 24: 1393–1403, 2010)

Androgens have well-defined roles in male reproduction (1) and prostate cancer (2, 3). In contrast, other than the obligatory role of testosterone as an estradiol precursor in steroidogenesis (4, 5), little is known about the direct involvement of androgens and androgen receptor (AR) actions in the female. Interestingly, global AR knockout (ARKO) female mice (6–8) are subfertile, have defective folliculogenesis, and ultimately develop premature ovarian failure. These AR-null mice have lower numbers of antral follicles, fewer corpora lutea (CL), and significantly higher rates of granulosa cell (GC) apoptosis. Moreover, these mice ovulate fewer oocytes after superovulation with gonadotropins. In contrast to the attenu-

ated follicle development observed in these AR-null mice with reduced androgen signaling, elevated androgen levels *in vivo*, as seen in animal models (9–11) of androgen excess and in the human disease of polycystic ovarian syndrome, is associated with excessive and unregulated follicle formation (12). Together, these animal and human examples suggest that androgen signaling through the AR may be necessary for normal follicle development and function, but that excessive androgen signaling might lead to abnormal follicular growth. However, these observations do not address where androgens are acting in the hypothalamic-pituitary-gonadal axis to regulate follicle growth and female fertility.

Abbreviations: AR, Androgen receptor; ARKO, AR-knockout; CL, corpora lutea; DHT, dihydrotestosterone; GAPDH, glyceraldehyde-3-phosphate dehydrogenase; GC, granulosa cell; GDF, growth differentiation factor; GVBD, germinal vesicle breakdown; IBMX, 3-isobutyl-1-methylxanthine; TUNEL, terminal deoxynucleotide transferase-mediated dUTP nick end labeling; WT, wild type.

ARs are expressed in all cell types of the ovarian follicle, including the oocyte, GCs, and theca cells. In addition, ARs are expressed in the hypothalamus and pituitary (13–15). Interestingly, AR signaling in all of these locations may be important for normal female fertility. For example, *in vitro* culture of GCs or follicles isolated from various species demonstrates AR-mediated stimulatory effects of androgens on proliferation and follicular development (16–23). With regard to oocytes, testosterone is capable of triggering mouse (24, 25) and porcine oocyte maturation (26, 27), most likely via the classical AR. Finally, potential hypothalamic/pituitary effects of androgens have been shown in sheep (9, 10), primate (11), and mouse (13) models in which *in utero* prenatal administration of androgens leads to abnormal LH pulse frequency and irregular reproductive cycles in postpubertal female offspring. In fact, androgens have been noted to suppress LH pulsatility in young women as well (28).

To begin to elucidate which AR-expressing cells are physiologically important contributors to ovarian function and fertility in female mice, we used the Cre-lox system to create transgenic mice lacking the AR specifically in either oocytes or GCs. We found that nearly all of the fertility phenotypes associated with the global ARKO mice are mirrored in the GC-, but not the oocyte-specific, ARKO mice, suggesting that AR signaling within the GCs of the ovary is a critical regulator of androgen-mediated follicle growth and development. In fact, local androgen actions in ovarian GCs, rather than in the pituitary or hypothalamus, may be the primary site of androgen-regulated fertility in female mice.

Results

Selective knockout of the AR in GCs

To generate GC-specific AR −/− mice we first crossed AR-loxP$^{flox/flox}$ females with anti-Müllerian hormone receptor type II (MisRII)cre males and thereafter, the MisRII-Cre/+;AR-loxP$^{flox/+}$ females were backcrossed with AR-loxP$^{flox/Y}$ males to generate female heterozygous control MisRII-Cre/+;AR-loxP$^{flox/+}$ mice and MisRII-Cre/+;AR-loxP$^{flox/flox}$ mice conditionally deleted for AR in GCs (Fig. 1A). To confirm selective knockout of AR in GCs, ovarian sections from 8- to 9-wk-old GC-specific AR −/− and wild-type (WT) animals were subjected to immunohistochemical analysis using an anti-AR antibody (Fig. 2A). As expected, the AR was expressed equally in the theca and GCs of WT mice (*upper panel*). In contrast, AR expression was intense in the theca, but not GCs in the GC-specific AR-null mice (GC AR −/−, *lower panel*). As reported previously (24, 27), AR expression was diffusely expressed in the oocytes of both WT and GC
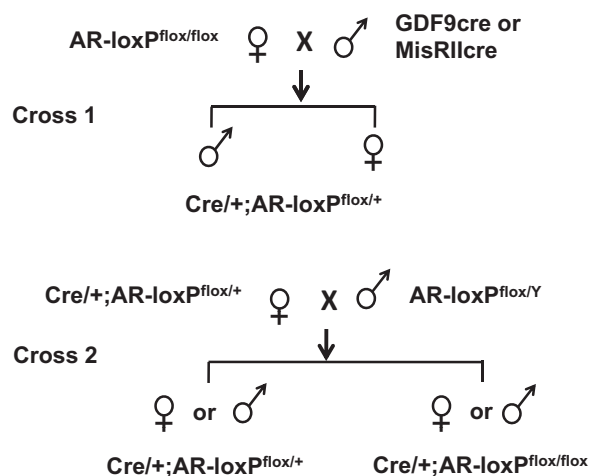


FIG. 1. Schematic diagram demonstrating the generation of GC- and oocyte-specific ARKO mouse. AR-loxP$^{flox/flox}$ females were crossed with GDF9cre males (for oocyte-specific −/−) or MisRIIcre males (for GC-specific −/−) and thereafter, the GDF9Cre/+ or MisRIICre/+;AR-loxP$^{flox/Y}$ females were backcrossed with AR-loxP$^{flox/Y}$ males to generate female heterozygous control GDF9- or MisRII-Cre/+;AR-loxP$^{flox/+}$ mice and GDF9- or MisRII-Cre/+;AR-loxP$^{flox/flox}$ mice conditionally deleted for AR in the oocyte and GC, respectively.

AR −/− mice. Further evidence for reduced AR expression in GCs was obtained from quantitative real-time PCR (Fig. 2B) and Western blot analysis (Fig. 2C), which showed that AR mRNA (Fig. 2B) and protein (Fig. 2C) expression in GCs isolated from GC-specific AR −/− mice was significantly ($P \leq 0.001$) lower than in GCs from WT and corresponding heterozygous littermates (Fig. 2B). Moreover, the equal expression of AR mRNA in the pituitary and hypothalamus isolated from WT, heterozygous, and AR-null mice (Fig. 2B) demonstrates the specificity of our GC-specific ARKO model and differentiates these mice from the global ARKO model. LnCAP and human embryonic kidney-293 cells were used as positive and negative controls, respectively.

To determine whether knockout of the AR using the MisRII promoter to drive Cre expression altered the gross morphology of the female ovary and uterus, we also examined the reproductive organs from 8- to 9-wk-old female mice at estrus. Under macroscopic examination, the ovaries and uteri of GC-specific ARKO animals appeared to be normal compared with AR +/− animals, suggesting no obvious morphological effects of ARs in these mice at this age (Supplemental Fig. 1 published on The Endocrine Society's Journals Online web site at http://mend.endojournals.org).

GC-specific ARKO female mice have reduced fertility and altered estrous cycling

To evaluate the reproductive performance of the GC-specific AR −/− mice, we conducted 12-wk long mating studies in 8- to 9-wk and 24- to 25-wk-old animals (Table 1). At 8–9 wk of age, WT and heterozygotic AR +/− mice
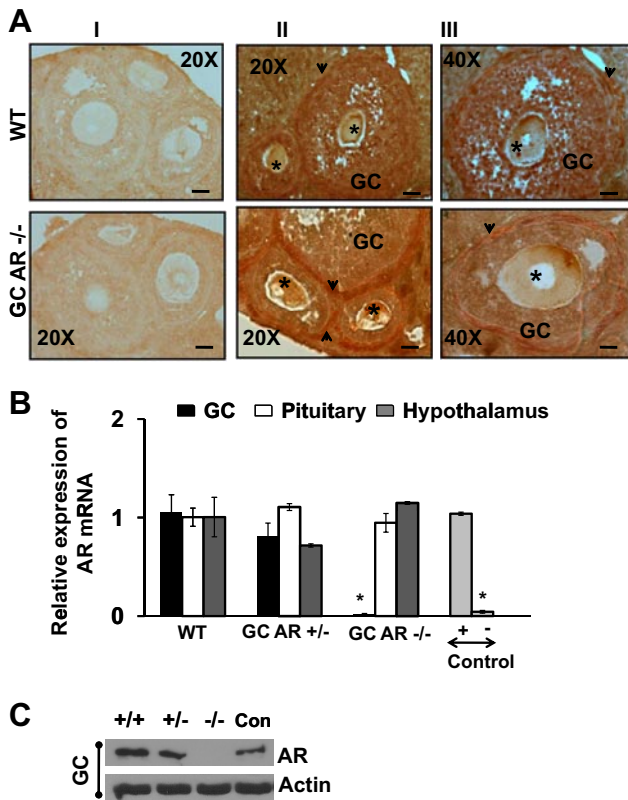
FIG. 2. Selective knockout of ARs in GCs. A, Representative photos of immunohistochemistry using an anti-AR antibody to detect AR expression in follicles isolated from 8- to 9-wk-old WT and GC-specific AR −/− mouse. The *arrowhead* and the *star* demonstrate AR theca cells and oocytes, respectively. Panel I represents the negative control (without primary antibody), and panels II and III represent follicles from WT and GC-specific AR −/− animals at ×20 (*bar*, 50 μm) and ×40 (*bar*, 100 μm) magnification, respectively. B, Graphic representation of AR mRNA transcripts in GCs, pituitary, and hypothalamus RNA extracts isolated from 8- to 9-wk-old WT, GC-specific AR +/−, and −/− animals. LnCAP and human embryonic kidney 293 cells were used as positive (+) and negative (−) controls, respectively. The mRNA levels were measured by quantitative real-time PCR and compared with control GAPDH mRNA expression using the $\Delta\Delta$Ct method. Results are represented as the amount relative to WT cells (mean ± SE, n = 4 mice per genotype). *, Using ANOVA, $P \leq 0.001$ for GC AR −/− *vs.* WT and GC AR +/− mice. C, Representative Western blot demonstrating the AR expression in GCs isolated from WT, GC-specific AR +/−, and −/− mice (n = 2 animals per genotype). LnCAP cells were used as positive control (Con). Similar results were observed in two separate experiments.

had 7.14 ± 0.9 and 6.96 ± 0.28 pups per litter, respectively, with both producing 3.5 ± 0.19 litters per female (Table 1). In contrast, 8- to 9-wk-old GC-specific AR −/− mice were substantially less fertile than AR +/− littermates and WT mice (Table 1), with a smaller average litter size (2.82 ± 0.2; $P \leq 0.01$) and average number of litters per female (2.13 ± 0.22; $P \leq 0.05$). Even more dramatic reductions in litter size and litter numbers of the GC-specific AR −/− mice relative to WT and heterozygotic mice were observed in 24- to 25-wk-old animals (Table 1).

To determine whether the reduced litter frequency in GC-specific AR −/− females was due in part to abnormal estrous cycling, vaginal smears from 8- to 9- and 24- to

25-wk-old mice (n = 5 for each age) were examined over the course of 1 month (Fig. 3). Despite having reduced litter frequency, the GC-specific AR −/− mice cycled normally, with normal estrous cycle lengths at 8–9 wk of age (Fig. 3A). In contrast, the GC-specific AR −/− female mice had longer estrous cycles in older (24–25 wk) mice relative to AR +/− females (7.33 ± 0.48 *vs.* 4.19 ± 0.31 d; $P \leq 0.05$). The longer estrous cycle in 24- to 25-wk-old GC AR −/− mice was due to increased duration of diestrus. Figure 3B demonstrates representative estrous cycling in one 24–25 wk-old GC-specific AR −/− and one AR +/− littermate. Overall, the GC AR −/− mice were in diestrus 75.6 ± 3.46% of the time, compared with 40.6 ± 3.28% for AR +/− littermates ($P \leq 0.05$; Fig. 3C).

GC-specific ARKO female mice ovulate fewer numbers of oocytes

To determine whether the reduced litter sizes and frequency seen in the GC-specific AR −/− female mice were due to lower ovulation rates, the numbers of ovulated oocytes in natural and superovulation conditions were counted. Figure 4A displays representative denuded oocytes and cumulus-oocyte complexes that were isolated from the oviducts of the animals after natural ovulation on the day of estrus. Results from five mice/genotype/age demonstrated that, irrespective of age (8–9 or 24–25 wk old), GC-specific AR −/− mice had significantly lower numbers of ovulated oocytes (2.4 ± 0.2 and 1 ± 0.3, respectively) compared with AR +/− littermates (6.8 ± 0.6 and 8.2 ± 0.9, respectively; $P \leq 0.01$) (Fig. 4B). In fact, the number of ovulated oocytes in the 24- to 25-wk-old mice was even lower than in the 8- to 9-wk-old mice, consistent with the smaller litter sizes observed in the older mice (Table 1). Notably, when subjected to a superovulation regime (Fig. 4C), the number of superovulated oocytes were comparable (18.2 ± 0.8 *vs.* 20.5 ± 1.4) in the 8- to 9-wk-old GC-specific AR −/− and AR +/− mice, but were significantly ($P \leq 0.01$) lower in the older (24–25 wk) GC-specific AR −/− mice relative to AR +/− mice (8.75 ± 1.2 *vs.* 18.6 ± 1.0). Together, these cycling and ovulation studies demonstrate that ablation of AR specifically in GCs is enough to cause decreased ovulation during normal cycling by 8–9 wk, with eventual disruption of the estrous cycle by 24–25 wk, both of which likely contribute to the observed reduced fertility in female mice.

Ovaries from GC-specific ARKO mice have age-dependent reduced folliculogenesis and increased follicular atresia

To gain further insight into the reduced fertility of the GC-specific AR −/− mice, ovarian morphology was studied

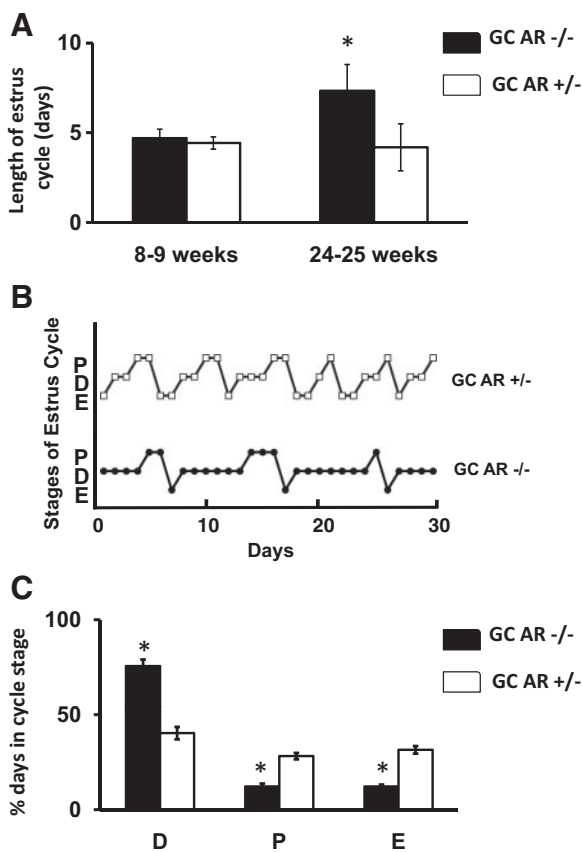**TABLE 1.** Female mice lacking AR expression in GCs have age-related reduced fertility

Genotype	n	Litter	Pups	Pups/litter	Litter/female
8- to 9-wk-old animals					
GC AR −/−	8	17	48	2.82 ± 0.2[a]	2.13 ± 0.22[b]
WT	8	28	200	7.14 ± 0.29	3.5 ± 0.19
GC AR +/−	8	28	195	6.96 ± 0.28	3.5 ± 0.19
24- to 25-wk-old animals					
GC AR −/−	6	10	16	1.6 ± 0.23[a]	1.66 ± 0.21[a]
WT	6	20	119	5.95 ± 0.25	3.33 ± 0.21
GC AR +/−	6	19	113	5.95 ± 0.42	3.17 ± 0.16

WT males were mated for 12 wk with 8- to 9-wk-old, or 24- to 25-wk-old WT and GC-specific AR −/− and +/− female animals. Both the number of litters and the number of pups per litter were determined. Data are represented as mean ± SE.
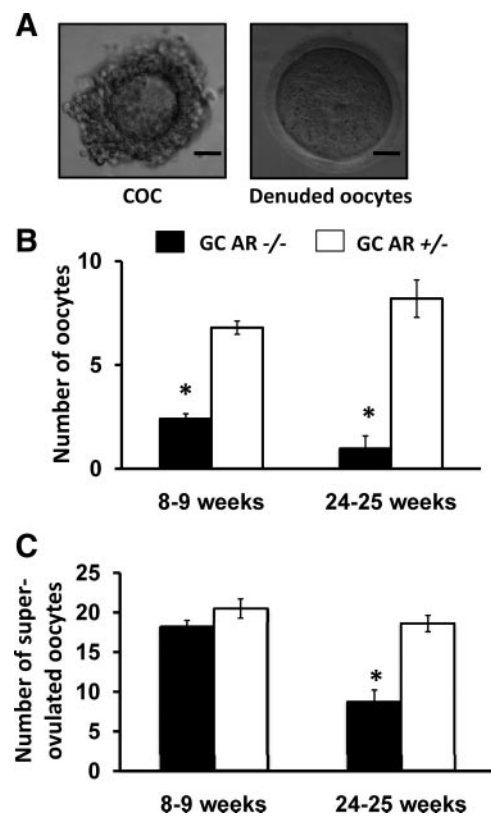[a] $P \leq 0.01$; [b] $P \leq 0.05$ for GC AR −/− vs. WT and GC AR +/− mice using ANOVA.

and compared with corresponding heterozygous littermates. Figure 5 demonstrates representative hematoxylin and eosin-stained ovarian sections from 4-wk (panel A), 8- to 9-wk (panel B), and 24- to 25-wk-old (panel C) GC-specific AR −/− and AR +/− mice. The distribution of growing follicles was almost identical when comparing 4-wk-old ovaries from GC-specific AR −/− vs. AR +/−
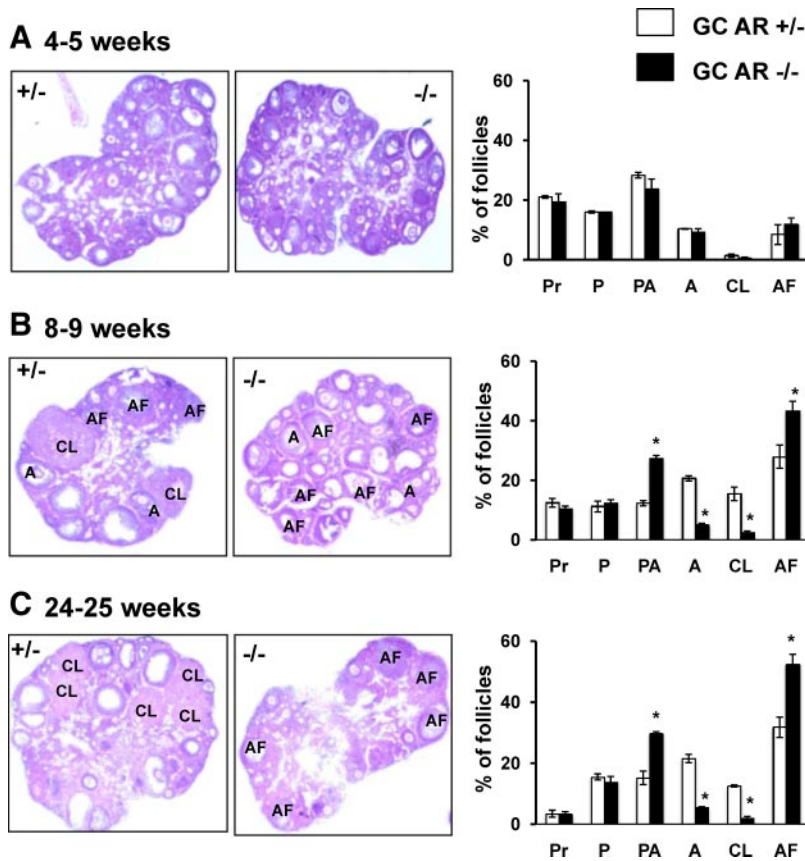
animals (Fig. 5A; n = 4 ovaries per genotype). Note that practically no CL could be identified at this age, consistent with the lack of ovulation in prepubertal mice. At 8–9 wk of

FIG. 4. GC-specific knockout of the AR results in reduced ovulation. A, Representative pictures of a cumulus-oocyte-complex (COC) and a denuded oocyte harvested from the oviduct and ampulla of a mouse after ovulation on the day of estrus (bar, 20 μm). B, Graphic representation of number of naturally ovulated oocytes in GC-specific AR −/− and AR +/− mice. Estrous cycles of 8- to 9-wk- and 24- to 25-wk-old female animals (n = 5 per genotype) were determined by vaginal smears for 2 wk and thereafter animals were killed at estrus. C, Number of superovulated oocytes in 8- to 9-wk- or 24- to 25-wk-old female GC-specific AR −/− and AR +/− mice (n = 5 per genotype). Mice were given a single ip injection of 5 U of pregnant mare serum gonadotropin followed 48 h later by 5 U of human chronic gonadotropin (Sigma). After 18 h, oocyte/cumulus masses were surgically isolated from the oviduct and ampulla and counted. Data are represented as mean ± SE (n = 5 mice). *, Using Student's t test $P \leq 0.01$ for GC AR −/− vs. GC AR +/− mice.

FIG. 3. Knockout of the AR in GCs disrupt estrous cyclicity. A, Graphic representation of average length of estrous cycle determined by vaginal smears taken daily over a period of 3–4 wk in 8- to 9-wk- or 24- to 25-wk-old GC-specific AR −/− and +/− animals. B, Representative estrous cycles in a single GC-specific AR +/− (upper) and AR−/− (lower) mice. C, Percent of days spent in each estrous cycle stage (D, diestrus; P, proestrus; E, estrus) in GC-specific AR +/− and −/− mice. Data are represented as mean ± SE (n = 5 mice). *, Using Student's t test, $P \leq 0.05$ for GC AR −/− vs. GC AR +/− mice.

FIG. 5. GC-specific AR −/− mice have reduced follicle progression and increased follicle atresia relative to AR −/− females. Representative hematoxylin and eosin-stained ovarian sections and statistical analysis of percentage of different types of follicles from 4- to 5-wk- (A), 8- to 9-wk- (B), and 24- to 25-wk-old (C) GC-specific AR +/− and AR −/− mice (n = 4 ovaries per genotype). Sections were taken at intervals of 30 μm, and 5 μm paraffin-embedded sections were mounted on slides. The types of follicles counted are: primordial (Pr), primary (P), preantral (PA), antral (A), corpus luteum (CL), and atretic follicles (AF). *, Using Student's t test, $P \leq 0.05$ for GC AR −/− vs. AR +/− mice.

age (Fig. 5B), GC-specific AR −/− ovaries had comparable percentages of primordial (Pr) and primary (P) follicles compared with AR +/− littermates. However, GC-specific AR −/− animals had significantly higher percentages of preantral (PA) follicles relative to AR +/− mice (27.2 ± 1.2% vs. 12.3 ± 0.9%), with significantly lower percentages of large antral (A) follicles (4.9 ± 0.9% vs. 20.6 ± 0.6%) and CL (2.5 ± 0.5% vs. 15.5 ± 2.3%). In addition, GC-specific AR −/− ovaries contained considerably more atretic follicles (AF) relative to AR +/− littermates (43.5 ± 3.1% vs. 27.9 ± 3.9% follicles). Further evidence of increased apoptosis in the GC-specific AR-null mice was also evident from higher rate of DNA fragmentation by TUNEL (terminal deoxynucleotide transferase-mediated dUTP nick end labeling) staining in ovaries isolated from 8- to 9-wk-old GC-specific AR-null relative to heterozygotic animals (Supplemental Fig. 2). This degenerated folliculogenesis was even more apparent in 24- to 25-wk-old GC-specific AR −/− mice (Fig. 5C), where the percentage of primordial and primary follicles in GC-specific AR −/− an-

imals remained similar to AR +/− animals, the percentage of antral follicles and corpus lutea remained lower in the GC-specific AR −/− mice, but the percentage of preantral and atretic follicles in the GC-specific AR −/− vs. AR +/− mice continued to rise (29.8 ± 0.5% preantral and 52.3 ± 3.4% atretic vs. 15.2 ± 2.2% preantral and 31.8 ± 3.3% atretic, respectively). These results suggest that many follicles in the GC-specific AR-null mice are halted in the preantral phase of development, where they then become atretic rather that develop into antral follicles that can be ovulated to produce corpus lutea. However, a subset of follicles still progress normally through follicular development. This interpretation likely explains the lower ovulation rates and premature ovarian failure seen in both GC-specific and global ARKO mice.
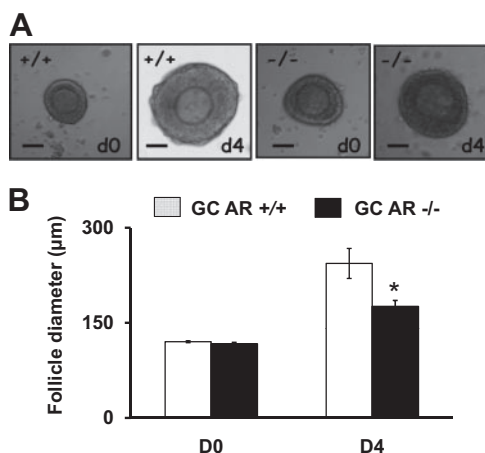
Follicles from GC-specific AR-null mice grow more slowly *in vitro*

To further demonstrate the importance of GC-specific ARs in follicular growth, we mechanically isolated preantral follicles from ovaries of 21-d-old GC-specific AR-null and WT female mice and cultured them *in vitro* for 4 d in the presence of FSH but absence of exogenous androgen (Fig. 6). Figure 6A shows representative follicles isolated from GC-specific AR −/− and WT animals, and Fig. 6B shows the average follicular diameter on d 0 (D0) and d 4 (D4) of culture. The diameter of the follicles isolated from WT animals nearly doubled over 4 d of culture. In contrast, the follicles isolated from GC-specific AR −/− mice grew at a significantly ($P \leq 0.05$) slower rate than the WT follicles (Fig. 6B). These data suggest that GC-specific ARs may regulate normal preantral follicular growth, perhaps through the endogenous production of androgens (29–33).

Selective knockout of ARs in the oocyte

To develop oocyte-specific ARKO mice we crossed AR-loxP$^{flox/flox}$ females with growth differentiation factor (GDF)9cre males and thereafter, the GDF9-Cre/+; AR-loxP$^{flox/+}$ females were backcrossed with AR-loxP$^{flox/Y}$ males to generate female heterozygous control GDF9-Cre/+; AR-loxP$^{flox/+}$ mice and GDF9-Cre/+;AR-loxP$^{flox/flox}$ mice conditionally deleted for AR in the oocyte (Fig. 1). Absence

A

B

FIG. 6. Ovarian follicles from GC-specific AR −/− mice grow more slowly *in vitro* than ovarian follicles from WT mice. Follicles of 100–120 μm diameter size were isolated from 21-d-old WT and GC AR −/− and cultured for 4 d in DMEM supplemented with 5 μg/ml of insulin, 5 μg/ml of transferrin, 5 ng/ml of sodium selenite, 1% penicillin-streptomycin, and 1 ng/ml of recombinant human FSH. Follicle diameters at the beginning (d0) and end (d4) of culture were measured by using the morphometric tool of the Zeiss Axioplan microscope (Zeiss). Representative pictures of follicles (panel A) and average diameter of follicles (panel B) (n = 25 follicles per genotype) isolated from GC-specific AR −/− and WT mice on d 0 and d 4 of culture. *, Using Student's *t* test, $P \leq 0.05$ for GC AR −/− *vs.* WT mice. *Bar*, 50 μm.

of AR mRNA in oocytes was determined by real-time PCR (Fig. 7). Oocytes were surgically harvested from the oviduct and ampulla of oocyte-specific AR −/−, corresponding heterozygous littermates (AR +/−), and WT animals on the day of the estrus, as well as manually isolated from individual follicles with a 30-gauge needle. GCs were removed mechanically and RNA collected from the denuded oocytes and GCs. AR mRNA was then quantified by real-time PCR. As shown in Fig. 7, relative expression of AR mRNA in the oocytes isolated from the oocyte-specific AR −/− mice was significantly lower compared with AR +/− and WT animals ($P \leq 0.01$). In contrast, AR mRNA expression in GCs iso-
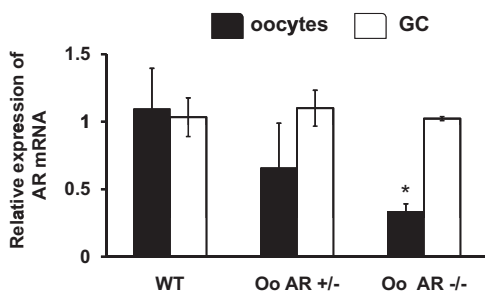

FIG. 7. Selective knockout of the AR in oocytes (Oo). Relative expression of AR mRNA in the oocytes and GCs isolated from 8- to 9-wk-old WT and oocyte-specific AR −/− and +/− mice. mRNA levels were measured by quantitative real-time PCR and compared with control GAPDH mRNA expression using the ΔΔCt method. Results are represented as mean ± SE (n = 4 per genotype). Approximately ≅120 oocytes per animal per genotype for each PCR were used. *, Using ANOVA, $P \leq 0.01$ for GC AR −/− *vs.* WT and GC AT +/− mice.

lated from the same animals was similar among all the genotypes (Fig. 7).

Oocytes with reduced AR expression do not mature in response to androgens

Several laboratories have now shown that steroids (androgens, progesterone, and estradiol) can promote oocyte maturation *in vitro* (21–24, 32–34). Studies using oocytes from progesterone receptor-null mice show that progestin-mediated oocyte maturation requires the classical progesterone receptor (34), whereas pharmacological studies suggest that androgen-mediated oocyte maturation occurs via the classical AR (21–24). To confirm these pharmacological studies using our genetic model, oocytes were isolated from the ovaries of unprimed 21-d-old oocyte-specific AR −/− and AR +/− mice to ensure that they had been exposed to minimal steroids before our studies. 3-isobutyl-1-methylxanthine (IBMX) was added to the media to reduce spontaneous maturation. Addition of dihydrotestosterone (DHT) to IBMX-treated oocytes isolated from AR +/− animals resulted in germinal vesicle breakdown (GVBD) in 64% of oocytes by 4 h and 82% by 8 h of treatment (Fig. 8). In contrast, DHT-induced GVBD in oocytes isolated from the oocyte-specific AR −/− animals was significantly ($P \leq 0.01$) lower (14% at 4 h and 28% at 8 h). Interestingly, irrespective of the genotype (oocyte-specific AR −/− or +/−) the progestin R5020 strongly promoted GVBD (Fig. 8). These results therefore provide genetic confirmation that androgens specifically promote oocyte maturation through AR signaling.
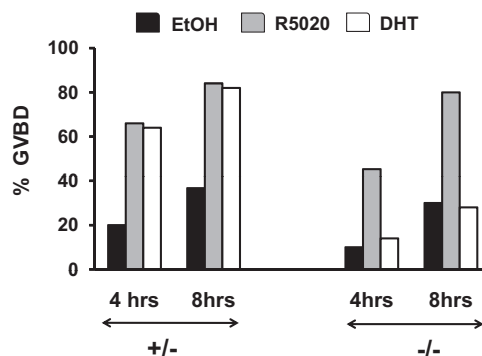
FIG. 8. Oocytes require AR expression for androgen- but not progestin-mediated maturation. Denuded oocytes isolated from 21-d-old oocyte-specific AR −/− and +/− mice (n = 2 animals per genotype) were treated with DHT (100 nM), R5020 (Promegestone, 250 nM), or ethanol (0.1%). Maturation (GVBD) of denuded oocytes was scored at 4 h and 8 h after treatment. Twenty-five oocytes per animal for each treatment were used for the experiment, and data are represented as the combined percent of oocytes that had undergone GVBD from two separate experiments. Data were analyzed using χ^2 test and $P \leq 0.01$ for DHT-treated oocytes isolated from oocyte-specific AR −/− *vs.* +/− mice.

TABLE 2. Female mice (8- to 9-wk-old animals) lacking AR expression in oocytes (Oo) have normal fertility

Genotype	n	Litter	Pups	Pups/litter	Litter/female
Oo AR −/−	6	20	139	6.95 ± 0.15	3.33 ± 0.21
WT	6	22	140	6.36 ± 0.38	3.7 ± 0.21
Oo AR +/−	6	21	149	7.1 ± 0.16	3.5 ± 0.22

Known fertile WT males were mated for 12 wk with 8- to 9-wk-old WT and Oo-specific AR −/− and +/− female animals. Both the number of litters and the number of pups per litter were determined. Data are represented as mean ± SE.
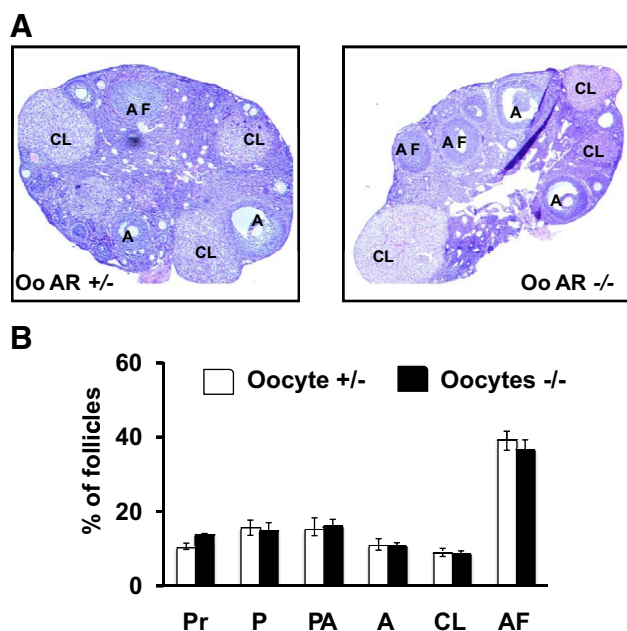
Oocyte-specific AR-null female mice have normal fertility and follicle morphology at 8–9 wk of age

Similar to GC-specific ARKO animals, we studied whether knockout of the AR in oocytes affected female fertility. Mating studies in 8- to 9-wk-old animals (Table 2) revealed that oocyte-specific AR −/− mice had normal litter sizes (6.95 ± 0.15) and litter numbers (3.33 ± 0.21) compared with WT (6.4 ± 0.38 pups per litter and 3.7 ± 0.21 litters per female) and AR +/− (7.1 ± 0.16 pups per litter and 3.5 ± 0.22 litters per female) animals. Furthermore, the ovarian morphology of 8- to 9-wk-old oocyte-specific ARKO mice was similar to AR +/− animals (Fig. 9). Unlike the GC-specific ARKO animals, ablation of ARs in the oocyte had no effect on follicular development at 8–9 wk, with no difference in the percentage of primordial (Pr), primary (P), preantral (PA), antral (A), atretic (AF) follicles, and CL between oocyte-specific AR −/− and AR +/− mice.

FIG. 9. Ovaries from oocyte (Oo)-specific AR +/− and AR −/− females are nearly identical. Representative hematoxylin and eosin-stained ovarian sections (*upper panel*) and statistical analysis of percentage of different type of follicles (*lower panel*) from 8- to 9-wk-old oocyte-specific AR +/− and −/− mice (n = 4 ovaries per genotype). Sections were taken at intervals of 30 μm and 5 μm paraffin-embedded sections were mounted on slides. The types of follicles counted are: primordial (Pr), primary (P), preantral (PA), antral (A), corpus luteum (CL), and atretic follicles (AF).

Discussion

Recent evidence suggests that androgen actions via the AR play an important role in female fertility (17, 18, 35, 36). Studies in global ARKO mouse models (6–8) demonstrate that these female mice are subfertile and develop premature ovarian failure with age. The aim of this study was to determine why the global AR-null females were subfertile, and which AR-expressing tissue(s), namely the hypothalamus, the pituitary, or the many cells within the ovary, were regulating fertility. The reproductive phenotypes of GC-specific ARKO mice observed in this study are very similar to the various total ARKO mouse models developed by Hu *et al.* (6), Shiina *et al.* (7), and Walters *et al.* (8), thereby demonstrating that subfertility in the global ARKO mice is likely due primarily to the functions of GC-specific ARs in normal follicular development.

The gene encoding the *AR* is located on the X chromosome, meaning that AR-null males are infertile. Thus, generating tissue-specific ARKO mice using classical knockout strategy is complex. To generate the GC-specific ARKO mice, we used mice in which exon 2 of the AR was floxed (37) and mated them with existing MisRIIcre mouse models. *MisRII* is expressed in the coelomic and mesenchyme epithelium surrounding the Müllerian duct as well as in the female urogenital ridges during embryogenesis (38, 39). More importantly, *MisRII* is also expressed in the GCs of both embryonic and adult ovaries (39). As evident from our immunohistochemical, real-time PCR, and Western blot studies, AR expression was specifically ablated in the granulosa, but not theca, cells using the MisRII cre recombinase. Because MisRII is also expressed in the uterus (38), AR expression may have also been ablated in the uterus, and this loss of AR function may have contributed to the observed subfertility. In fact, Hu *et al.* (6) described changes in uterine morphology in their global AR-null mice. However, we did not observe any differences in the uterogenital tracts of the GC-specific AR −/− (Supplemental Fig. 1), consistent with results in the global ARKO mouse published by Shiina *et al.* (7). This suggests that the reproductive defects and subfertility seen in both our mice and the global AR-null mice developed by Shiina *et al.* (7) are not due to changes in the uterus.

Why then do we see reduced fertility and premature ovarian failure in the global and GC-specific ARKO mice? Studies in both mouse models reveal low numbers of antral follicles, ovulated oocytes, and CLs, with a high rate of follicular atresia (6, 7). In addition, we observed that knockout of AR expression specifically in GCs resulted in accumulation of higher numbers of small preantral follicles. This accumulation was not due to increased recruitment of primordial follicles because the percentage of primordial and primary follicles in GC-specific AR −/− and +/− were similar at 8- to 9-wk and 24- to 25-wk-old mice. In accordance with the *in vivo* observation of preantral follicle accumulation, *in vitro* follicle culture showed that preantral follicles from GC-specific ARKO mice grew at a slower rate than WT follicles. This observation is consistent with *in vitro* pharmacological studies showing that AR antagonists slow mouse follicle growth (29, 30), androgen-induced porcine GC proliferation (20, 23), and androgen-induced primary to secondary transition in bovine follicles (35). Moreover, pharmacological inhibition of ARs both *in vivo* and *in vitro* decreases the diameter of mouse follicles stimulated by androgens (16) and induces rat GC degeneration and follicular apoptosis (40). Together the pharmacological studies along with our current genetic experiments strongly suggest that AR signaling in GCs is necessary for normal follicular growth and progression beyond preantral stage. When AR signaling is blocked or eliminated, preantral follicles cannot progress to antral follicles and, instead, are subjected to increased rate of atresia. This process would explain the lower number of antral follicles and CLs, as well as the lower number of ovulated oocytes and the subfertility, seen in the GC-specific ARKO mice. In addition, the more rapid follicular atresia might explain the premature ovarian failure seen in global and GC-specific AR-null mice.

Previous studies (6) have proposed that the longer estrous cycles correlating with reduced fertility in the total ARKO mice may be due to defects in androgen signaling within the hypothalamus and pituitary (41). However, here we show that the GC-specific ARKO mice had similarly lengthened estrous cycles, suggesting that the observed irregularity in cycling may be due, in large part, to a lack of androgen effects in the ovary, specifically in GCs. In fact, the global ARKO mice have lower progesterone levels compared with WT animals (42), most likely due to fewer CLs (as also observed here in the GC-specific ARKO mice). Furthermore, many models of primary premature ovarian failure have similarly demonstrated an increase in diestrus length (6, 43, 44). Together, these observations implicate reduced ovarian rather than central androgen signaling as the primary cause of altered cycling, with reduced CL formation leading to a loss of progesterone-mediated negative feedback on the hypothalamus-pituitary axis. Interestingly, central defects in androgen signaling have also been implicated as the primary regulators of infertility in models and diseases of androgen excess, including polycystic ovarian syndrome (9–15). However, we postulate that, based on our data, primary androgen signaling in the ovary may be equally important in the overall regulation of female fertility.

In contrast to the GC-specific ARKO mice, knockout of AR expression in oocytes has no effect on female fertility. However, one caveat is that the GDF9 promoter, and therefore the Cre enzyme, is not fully activated in primordial follicles (45, 46); thus, the effects of oocyte-specific AR expression on very early follicle development cannot be examined with this particular mouse model.

Interestingly, we (24, 25, 47, 48) and others (26, 27, 49–51) have previously shown that progestins and androgens can promote oocyte maturation. For progesterone, both pharmacological (25, 50) and genetic evidence (with progesterone receptor-null mice) (34) implicate the classical progesterone receptor is the regulator of progestin-mediated mouse oocyte maturation, whereas immunohistochemical (25) and pharmacological (24, 27) evidence implicate the classical AR as the mediator of androgen-induced maturation. Here we confirm in a genetic model that the classical AR is indeed necessary for androgen-, but not progestin-mediated, oocyte maturation *in vitro*. However, because follicular development and overall fertility of the oocyte-specific ARKO mice were normal at 8–9 wk compared with heterozygous littermates, androgen-induced oocyte maturation does not appear to be an essential process (although fertility could be compromised at a later age not examined in this study). In contrast, whether the AR signaling in the oocyte becomes important under conditions of androgen excess like polycystic ovarian syndrome is still not known.

In summary, this study differentiates the role of GC and oocyte AR in female fertility, demonstrating that most of the observed reproductive phenotypes in the complete AR-null mice are due to GC-specific AR. Furthermore, this study demonstrates that AR signaling in GCs, but not oocytes, regulates female fertility, perhaps by controlling preantral follicle growth and development to antral follicles, while preventing follicular atresia.

Materials and Methods

Generation of GC- and oocyte-specific ARKO mice

All mouse studies were approved by the University Committee on Animal Resources at the University of Rochester and conform to the Guidelines for the Care and Use of Laboratory Animals put out by the National Institutes of Health.

To generate GC- and oocyte-specific ARKO mice, we used mice in which exon 2 of the AR was floxed (37) and then mated them with existing GDF9cre (for oocyte-specific −/−) or Mis-RIIcre (for GC-specific −/−) mice (Fig. 1) (38, 39, 46). We first crossed AR-loxP$^{flox/flox}$ females with GDF9-cre or MisRII-cre males. Thereafter, the GDF9- or MisRII-Cre/+;AR-loxP$^{flox/+}$ females were backcrossed with AR-loxP$^{flox/Y}$ males to generate female heterozygous control GDF9- or MisRII-Cre/+;AR-lox-P$^{flox/+}$ mice and GDF9- or MisRII-Cre/+;AR-loxP$^{flox/flox}$ mice conditionally deleted for AR in the oocyte and GC, respectively (Fig. 1A). Genomic DNA was isolated from 10- to 12-d-old animals, and PCR genotyping with appropriate primers was used to identify mice with WT, floxed, and cre transgene, revealing bands of 855, 952, and 404 bp, respectively. The ARflox mice were a gracious gift from Dr. Guido Verhoeven, Catholic University of Leuven, Belgium whereas the GDF9cre and Mis-RIIcre mice were obtained from Dr. Martin Matzuk, Baylor College of Medicine.

Immunohistochemistry

The ABC method (Vector Laboratories, Burlingame, CA) was used according to the manufacturer's instructions for the immunohistochemical analysis of ovarian sections from 8- to 9-wk-old GC-specific ARKO and WT animals. Briefly, paraffin-embedded sections were dewaxed in xylene and ethanol and then subjected to antigen retrieval by boiling in 0.1 M citrate buffer (pH 6) in a microwave for 30 min. The cooled sections were then incubated with 0.3% hydrogen peroxide for 30 min for quenching of endogenous peroxidase and then permeabilized with 1% Triton-X100 in water for 5 min. The slides were blocked with 1.5% blocking serum (normal goat serum) from Vectastain *elite* ABC kit (Vector Laboratories, Inc.) for 30 min, and thereafter the slides were incubated with anti-AR rabbit polyclonal antibody (1:50; Santa Cruz Biotechnology, Inc., Santa Cruz, CA) in the blocking serum overnight at 4 C. Control slides were incubated with the blocking serum without primary antibody. Sections were incubated with biotinylated goat anti-rabbit IgG (1:100; Vectastain *elite* ABC kit, Vector Laboratories) for 1 h at room temperature, washed in PBS, and incubated in avidin-biotinylated horseradish peroxidase (Vectastain *elite* ABC kit) for 30 min at room temperature. Then the sections were washed and developed with solution containing diamino-benzidine + hydrogen peroxide solution (DAB substrate kit for peroxidase; Vector laboratories). The sections were counter stained with hematoxylin and eosin, dehydrated with series of ethanol and xylene, washed, and mounted with VectaMount (Vector Laboratories).

Western blot analysis

Western blots were performed as described previously (52). Samples were separated on 7.5% SDS-polyacrylamide gels for AR. Primary antibodies used were: antirabbit AR (1:1000 dilution; Santa Cruz Biotechnology) and anti-β-actin (1:5000; Millipore Corp., Bedford, MA).

TUNEL assay

TUNEL assay was performed using ApopTag Plus Peroxidase *In Situ* Apoptosis detection kit from Chemicon International (Temecula, CA) as per the manufacturer's instructions.

Fertility testing and estrous cycle tracking

To evaluate the reproductive performance of the GC- or oocyte-specific ARKO females, we conducted a continuous mating study for 12 wk using 8- to 9-wk (n = 8 for GC- and n = 6 for oocyte-specific ARKO animals) or 24- to 25-wk-old (n = 6, only for GC-specific AR-knockout) animals. One GC- or oocyte-specific ARKO female, one heterozygous littermate, or one WT female mouse, was housed with one 6- to 10-wk-old fertile WT male mouse. The male was replaced every 2 wk with another fertile male. Cages were monitored daily, and the number of pups and litters was recorded. Estrous cycle (proestrus, estrus, and diestrus) of 8- to 9-wk or 24- to 25-wk-old (only for GC-specific ARKO) animals was determined by vaginal smears taken daily for 3–4 wk (53).

RNA extraction and real-time PCR

Intact follicles were isolated from ovaries of either GC- or oocyte-specific ARKO females, corresponding heterozygous female littermates, and WT female animals with a 30-gauge needle (n = 4 per genotype). Thereafter the follicles were punctured with a 26-gauge needle to release the GCs into the media, and GCs were collected by centrifugation. For oocyte isolation, oocytes were surgically isolated from the oviduct and the ampulla of animals on the day of the estrus as well as manually isolated from individual follicles with a 30-gauge needle. Oocytes were denuded with gentle pipetting with pulled-glass pasteur pipettes and ≅120 oocytes per animal per genotype for each PCR were used. RNA from GC, oocytes, pituitary, and hypothalamus were isolated by using RNeasy mini kit (QIAGEN, Valencia, CA) according to the manufacturer's instructions, and the level of AR and glyceraldehyde-3-phosphate dehydrogenase (GAPDH) expression was analyzed by Δ/Δ Ct method using Taqman gene expression assay primers (Assay identification no. Mm00442688_m1-Ar and Mm03302249_g1-GAPDH; Applied Biosystems, Foster City, CA) and ABI StepOne plus real-time PCR machine.

Oocyte count from natural- and superovulation

For natural ovulation, estrous cycling of 8- to 9-wk- and 24- to 25-wk-old female GC-specific ARKO and heterozygous animals (n = 5) was determined by vaginal smears for 2 wk after which animals were killed at estrus. For superovulation, 8- to 9-wk- or 24- to 25-wk-old female GC-specific ARKO and heterozygous littermate mice (n = 5) were given a single ip injection of 5 U of pregnant mare serum gonadotropin (Sigma, St. Louis, MO) followed 48 h later by 5 U of human chorionic gonadotropin (Sigma). After an additional 18 h, oocyte/cumulus masses were surgically isolated from the oviduct and ampulla and counted.

Histology

Ovaries from 4-wk-old, 8- to 9-wk-old, and 24- to 25-wk-old GC-specific or oocyte-specific (only 8–9 wk old) ARKO and heterozygous littermates (n = 4 ovaries per genotype per age) were fixed in 4% paraformaldehyde at 4 C and then paraffin embedded. Thereafter, 5-μm sections were taken at 30-μm intervals, mounted on slides, and subjected to hematoxylin and eosin staining for histological examination by light microscopy. Follicle numbers were evaluated as: 1) primordial follicles, identified by an oocyte partially or completely encapsulated by flattened squamous cells; 2) primary follicles, single layer of cuboidal GCs around the oocyte; 3) secondary-tertiary follicles (preantral), two layers or more of cuboidal GCs (no antrum); 4) antral follicles, presence of an antrum; and 5) CL. Follicles were

considered atretic based on any of the two criteria: Three or more pyknotic nuclei or atretic bodies (depending on the follicle type) in GC layers or follicular antrum, GCs pulling away from basement membrane, broken basement membrane, uneven GC layer, and nonintact oocyte or nucleus. The data are represented as percentage of follicles.

In vitro follicle culture

Follicles of 100–120 μm size with two or three layers of GCs, an intact basal lamina, and few theca cells (approximately pre-antral follicles) were manually isolated from 21-d-old GC-specific ARKO and WT animals. The follicles were then cultured at 37 C in a humidified atmosphere (5% CO_2 and 95% air) for 4 d in DMEM supplemented with 5 μg/ml of insulin, 5 μg/ml of transferin, 5 ng/ml of sodium selenite, 1% penicillin-streptomycin, and 1 ng/ml of recombinant human FSH (29, 30, 32). The maximal follicle diameter at the beginning (D0) and end (D4) of culture was measured by using the morphometric tool of the Zeiss Axioplan microscope (Carl Zeiss, Inc., Thornwood, NY). The data represented here are the average diameter of 25 follicles per genotype isolated from GC-specific ARKO and WT animals (16, 29).

Oocyte maturation assay

Oocyte maturation assay was performed as described previously (24, 25). Briefly, both the ovaries from unprimed 21-d-old GC-specific ARKO and corresponding heterozygous littermates (n = 2 animals per genotype) were placed in M2 medium (Chemicon) containing 200 μM IBMX (Calbiochem, La Jolla, CA) and oocytes were manually harvested with 30-gauge needles. Oocytes were denuded with gentle pipetting with pulled-glass pasteur pipettes, washed with M2 medium, allocated into four-well culture dishes containing M16/IBMX, and kept at 37 C in a humidified atmosphere (5% CO_2). Oocytes were treated with either DHT (100 nM, Steraloids, Inc., Newport, RI), R5020, Promegestone (250 nM), or ethanol (0.1%). Twenty-five oocytes per animal per treatment were used for the experiment, and maturation (GVBD) of denuded oocytes was scored at 4 h and 8 h. The oocyte maturation assay was conducted twice, separately for each pair (GC AR −/− and +/−, and data are represented as an average percent of GVBD.

Statistical analysis

The RT-PCR experiments and fertility tests were analyzed by ANOVA whereas Chi-Square test was used for the analysis of the oocyte maturation data. For the remainder of the experiments, results were analyzed using Students's t test. A value of $P \leq 0.05$ was considered significant.

Acknowledgments

We thank Dr. Guido Verhoeven (Catholic University of Leuven, Belgium) and Karel De Gendt (University of California, San Diego, CA) for supplying us with the ARflox mice; Dr. Michael McPhaul (University of Texas Southwestern Medical Center, Dallas, TX) for his help starting this project; Dr. Martin Matzuk (Baylor College of Medicinie, Houston, TX) for supplying us with the two Cre mouse lines; and Louise Hartson (University of Rochester, Rochester, NY) for helping us with the histological sectioning.

References

1. Quigley CA, De Bellis A, Marschke KB, el-Awady MK, Wilson EM, French FS 1995 Androgen receptor defects: historical, clinical, and molecular perspectives. Endocr Rev 16:271–321
2. Lange CA, Gioeli D, Hammes SR, Marker PC 2007 Integration of rapid signaling events with steroid hormone receptor action in breast and prostate cancer. Annu Rev Physiol 69:171–199
3. Xu Y, Chen SY, Ross KN, Balk SP 2006 Androgens induce prostate cancer cell proliferation through mammalian target of rapamycin activation and post-transcriptional increases in cyclin D proteins. Cancer Res 66:7783–7792
4. Hillier SG, Whitelaw PF, Smyth CD 1994 Follicular oestrogen synthesis: the 'two-cell, two-gonadotrophin' model revisited. Mol Cell Endocrinol 100:51–54
5. Simpson ER 2002 Aromatization of androgens in women: current concepts and findings. Fertil Steril 77(Suppl 4):S6–S10
6. Hu YC, Wang PH, Yeh S, Wang RS, Xie C, Xu Q, Zhou X, Chao HT, Tsai MY, Chang C 2004 Subfertility and defective folliculogenesis in female mice lacking androgen receptor. Proc Natl Acad Sci USA 101:11209–11214
7. Shiina H, Matsumoto T, Sato T, Igarashi K, Miyamoto J, Takemasa S, Sakari M, Takada I, Nakamura T, Metzger D, Chambon P, Kanno J, Yoshikawa H, Kato S 2006 Premature ovarian failure in androgen receptor-deficient mice. Proc Natl Acad Sci USA 103:224–229
8. Walters KA, Allan CM, Jimenez M, Lim PR, Davey RA, Zajac JD, Illingworth P, Handelsman DJ 2007 Female mice haploinsufficient for an inactivated androgen receptor (AR) exhibit age-dependent defects that resemble the AR null phenotype of dysfunctional late follicle development, ovulation, and fertility. Endocrinology 148: 3674–3684
9. Smith P, Steckler TL, Veiga-Lopez A, Padmanabhan V 2009 Developmental programming: differential effects of prenatal testosterone and dihydrotestosterone on follicular recruitment, depletion of follicular reserve, and ovarian morphology in sheep. Biol Reprod 80: 726–736
10. Abbott DH, Padmanabhan V, Dumesic DA 2006 Contributions of androgen and estrogen to fetal programming of ovarian dysfunction. Reprod Biol Endocrinol 4:17
11. Abbott DH, Dumesic DA, Eisner JR, Colman RJ, Kemnitz JW 1998 Insights into the development of polycystic ovary syndrome (PCOS) from studies of prenatally androgenized female rhesus monkeys. Trends Endocrinol Metab 9:62–67
12. Ehrmann DA 2005 Polycystic ovary syndrome. N Engl J Med 352: 1223–1236
13. Sullivan SD, Moenter SM 2004 Prenatal androgens alter GABAergic drive to gonadotropin-releasing hormone neurons: implications for a common fertility disorder. Proc Natl Acad Sci USA 101:7129–7134
14. Sullivan SD, Moenter SM 2005 GABAergic integration of progesterone and androgen feedback to gonadotropin-releasing hormone neurons. Biol Reprod 72:33–41
15. Pielecka J, Quaynor SD, Moenter SM 2006 Androgens increase gonadotropin-releasing hormone neuron firing activity in females and interfere with progesterone negative feedback. Endocrinology 147:1474–1479
16. Wang H, Andoh K, Hagiwara H, Xiaowei L, Kikuchi N, Abe Y,

Yamada K, Fatima R, Mizunuma H 2001 Effect of adrenal and ovarian androgens on type 4 follicles unresponsive to FSH in immature mice. Endocrinology 142:4930–4936

17. Weil S, Vendola K, Zhou J, Bondy CA 1999 Androgen and follicle-stimulating hormone interactions in primate ovarian follicle development. J Clin Endocrinol Metab 84:2951–2956

18. Vendola KA, Zhou J, Adesanya OO, Weil SJ, Bondy CA 1998 Androgens stimulate early stages of follicular growth in the primate ovary. J Clin Invest 101:2622–2629

19. Cárdenas H, Herrick JR, Pope WF 2002 Increased ovulation rate in gilts treated with dihydrotestosterone. Reproduction 123:527–533

20. Vendola K, Zhou J, Wang J, Famuyiwa OA, Bievre M, Bondy CA 1999 Androgens promote oocyte insulin-like growth factor I expression and initiation of follicle development in the primate ovary. Biol Reprod 61:353–357

21. Hillier SG, Tetsuka M 1997 Role of androgens in follicle maturation and atresia. Baillieres Clin Obstet Gynaecol 11:249–260

22. Hickey TE, Marrocco DL, Amato F, Ritter LJ, Norman RJ, Gilchrist RB, Armstrong DT 2005 Androgens augment the mitogenic effects of oocyte-secreted factors and growth differentiation factor 9 on porcine granulosa cells. Biol Reprod 73:825–832

23. Hickey TE, Marrocco DL, Gilchrist RB, Norman RJ, Armstrong DT 2004 Interactions between androgen and growth factors in granulosa cell subtypes of porcine antral follicles. Biol Reprod 71:45–52

24. Gill A, Jamnongjit M, Hammes SR 2004 Androgens promote maturation and signaling in mouse oocytes independent of transcription: a release of inhibition model for mammalian oocyte meiosis. Mol Endocrinol 18:97–104

25. Jamnongjit M, Gill A, Hammes SR 2005 Epidermal growth factor receptor signaling is required for normal ovarian steroidogenesis and oocyte maturation. Proc Natl Acad Sci USA 102:16257–16262

26. Li M, Schatten H, Sun QY 2009 Androgen receptor's destiny in mammalian oocytes: a new hypothesis. Mol Hum Reprod 15:149–154

27. Li M, Ai JS, Xu BZ, Xiong B, Yin S, Lin SL, Hou Y, Chen DY, Schatten H, Sun QY 2008 Testosterone potentially triggers meiotic resumption by activation of intra-oocyte SRC and MAPK in porcine oocytes. Biol Reprod 79:897–905

28. Blank SK, McCartney CR, Helm KD, Marshall JC 2007 Neuroendocrine effects of androgens in adult polycystic ovary syndrome and female puberty. Semin Reprod Med 25:352–359

29. Murray AA, Gosden RG, Allison V, Spears N 1998 Effect of androgens on the development of mouse follicles growing in vitro. J Reprod Fertil 113:27–33

30. Spears N, Murray AA, Allison V, Boland NI, Gosden RG 1998 Role of gonadotrophins and ovarian steroids in the development of mouse follicles in vitro. J Reprod Fertil 113:19–26

31. Lenie S, Smitz J 2009 Functional AR signaling is evident in an in vitro mouse follicle culture bioassay that encompasses most stages of folliculogenesis. Biol Reprod 80:685–695

32. Lenie S, Cortvrindt R, Adriaenssens T, Smitz J 2004 A reproducible two-step culture system for isolated primary mouse ovarian follicles as single functional units. Biol Reprod 71:1730–1738

33. Orisaka M, Jiang JY, Orisaka S, Kotsuji F, Tsang BK 2009 Growth differentiation factor 9 promotes rat preantral follicle growth by up-regulating follicular androgen biosynthesis. Endocrinology 150: 2740–2748

34. Deng J, Carbajal L, Evaul K, Rasar M, Jamnongjit M, Hammes SR 2009 Nongenomic steroid-triggered oocyte maturation: of mice and frogs. Steroids 74:595–601

35. Yang MY, Fortune JE 2006 Testosterone stimulates the primary to secondary follicle transition in bovine follicles in vitro. Biol Reprod 75:924–932

36. Walters KA, Allan CM, Handelsman DJ 2008 Androgen actions and the ovary. Biol Reprod 78:380–389

37. De Gendt K, Swinnen JV, Saunders PT, Schoonjans L, Dewerchin M, Devos A, Tan K, Atanassova N, Claessens F, Lécureuil C, Heyns W, Carmeliet P, Guillou F, Sharpe RM, Verhoeven G 2004 A Sertoli cell-selective knockout of the androgen receptor causes spermatogenic arrest in meiosis. Proc Natl Acad Sci USA 101:1327–1332

38. Arango NA, Szotek PP, Manganaro TF, Oliva E, Donahoe PK, Teixeira J 2005 Conditional deletion of β-catenin in the mesenchyme of the developing mouse uterus results in a switch to adipogenesis in the myometrium. Dev Biol 288:276–283

39. Teixeira J, Maheswaran S, Donahoe PK 2001 Mullerian inhibiting substance: an instructive developmental hormone with diagnostic and possible therapeutic applications. Endocr Rev 22:657–674

40. Peluso JJ, Charlesworth J, England-Charlesworth C 1981 Role of estrogen and androgen in maintaining the preovulatory follicle. Cell Tissue Res 216:615–624

41. Walters KA, McTavish KJ, Seneviratne MG, Jimenez M, McMahon AC, Allan CM, Salamonsen LA, Handelsman DJ 2009 Subfertile female androgen receptor knockout mice exhibit defects in neuroendocrine signaling, intraovarian function, and uterine development but not uterine function. Endocrinology 150:3274–3282

42. Yeh S, Hu YC, Wang PH, Xie C, Xu Q, Tsai MY, Dong Z, Wang RS, Lee TH, Chang C 2003 Abnormal mammary gland development and growth retardation in female mice and MCF7 breast cancer cells lacking androgen receptor. J Exp Med 198:1899–1908

43. Andreu-Vieyra C, Chen R, Matzuk MM 2008 Conditional deletion of the retinoblastoma (Rb) gene in ovarian granulosa cells leads to premature ovarian failure. Mol Endocrinol 22:2141–2161

44. Altuntas CZ, Johnson JM, Tuohy VK 2006 Autoimmune targeted disruption of the pituitary-ovarian axis causes premature ovarian failure. J Immunol 177:1988–1996

45. Elvin JA, Yan C, Matzuk MM 2000 Oocyte-expressed TGF-beta superfamily members in female fertility. Mol Cell Endocrinol 159:1–5

46. Reddy P, Liu L, Adhikari D, Jagarlamudi K, Rajareddy S, Shen Y, Du C, Tang W, Hämäläinen T, Peng SL, Lan ZJ, Cooney AJ, Huhtaniemi I, Liu K 2008 Oocyte-specific deletion of Pten causes premature activation of the primordial follicle pool. Science 319: 611–613

47. Jamnongjit M, Hammes SR 2005 Oocyte maturation: the coming of age of a germ cell. Semin Reprod Med 23:234–241

48. Jamnongjit M, Hammes SR 2006 Ovarian steroids: the good, the bad, and the signals that raise them. Cell Cycle 5:1178–1183

49. Yamashita Y, Shimada M, Okazaki T, Maeda T, Terada T 2003 Production of progesterone from de novo-synthesized cholesterol in cumulus cells and its physiological role during meiotic resumption of porcine oocytes. Biol Reprod 68:1193–1198

50. Ning G, Ouyang H, Wang S, Chen X, Xu B, Yang J, Zhang H, Zhang M, Xia G 2008 3′,5′-cyclic adenosine monophosphate response element binding protein up-regulated cytochrome P450 lanosterol 14α-demethylase expression involved in follicle-stimulating hormone-induced mouse oocyte maturation. Mol Endocrinol 22:1682–1694

51. Borman SM, Chaffin CL, Schwinof KM, Stouffer RL, Zelinski-Wooten MB 2004 Progesterone promotes oocyte maturation, but not ovulation, in nonhuman primate follicles without a gonadotropin surge. Biol Reprod 71:366–373

52. Evaul K, Hammes SR 2008 Cross-talk between G protein-coupled and epidermal growth factor receptors regulates gonadotropin-mediated steroidogenesis in Leydig cells. J Biol Chem 283:27525–27533

53. Goldman JM, Murr AS, Cooper RL 2007 The rodent estrous cycle: characterization of vaginal cytology and its utility in toxicological studies. Birth Defects Res B Dev Reprod Toxicol 80:84–97